

CLOUD CHAMBER INVESTIGATIONS IN THE CORES OF EXTENSIVE AIR SHOWERS

O. I. DOVZHENKO, S. I. NIKOL'SKII, and I. V. RAKOBOL'SKAYA

P. N. Lebedev Physics Institute, Academy of Sciences, U.S.S.R.

Submitted to JETP editor June 14, 1958

J. Exptl. Theoret. Phys. (U.S.S.R.) **36**, 17-23 (January, 1959)

The results of an experimental investigation of the structure of the cores of extensive air showers are presented. Photographs of the cores of extensive air showers traversing the chamber are shown.

INTRODUCTION

THE study of extensive air showers (EAS) has become of increasing interest in recent years. This is due to the fact that the investigation of the composition and energy distribution of the shower particles, and also of the Cerenkov light pulses associated with the EAS, makes it possible, in principle, to study the interaction of ultra-high-energy particles ($> 10^{13}$ ev). From this point of view, it is especially important to study the central region of the shower — its core. However, the core is the least known region, and at present it is even impossible to indicate its dimensions. The core structure might be understood through a detailed study of the energy fluxes and the energy spectra of particles contained in the central region of the EAS. In that respect, the study of the air-shower cores by means of a large number of ionization chambers yields rich quantitative material. More visual although less statistically founded data on the structure of shower cores can be obtained with cloud chambers. This method was used in the present experiment.

The measurements were carried out at sea level in Moscow in 1957.

1. MEASUREMENT PROCEDURE

For an effective observation of the cores of EAS, we used a rectangular cloud chamber with a special triggering system. This system selected only those showers in which the particle density, recorded by means of counters placed above the cloud chamber, was larger than the density of shower particles recorded by groups of counters placed further away. The position of the master group of counters can be seen in the general diagram of the array (see Fig. 1).

Groups 1 to 4 contain 12 counters each, and groups 5 and 6 contain 18 counters. The area of

each counter was $\sigma = 100 \text{ cm}^2$ in the first series of measurements, and $\sigma = 330 \text{ cm}^2$ in the second series. The amplitude of the pulse in each group was proportional to the total number of discharged counters in it. If we denote the number of discharged counters in the i -th group by m_i , then the condition of recording EAS can be given by the formula

$$\sum_{i=5}^6 m_i - \sum_{j=1}^4 m_j \geq \xi, \quad m_5 \geq 2, \quad m_6 \geq 2.$$

The minimum value of ξ was 6 and 9 for the experiments with master counters 100 cm^2 and 330 cm^2 in area, respectively. Local showers produced in the cover above the array were practically excluded by the requirement of discharges in not less than 2 counters of each of the groups 5 and 6.

For the determination of the total number of particles in the recorded showers, we used a hodoscopic array consisting of 6 groups of counters with an area $\sigma = 100 \text{ cm}^2$ each. Each group contained 24 counters (group 7 — 12 in Fig. 1). The resolving time of the master system amounted to about $10 \mu \text{ sec}$.

The cloud chamber used¹ measured $60 \times 60 \times 30 \text{ cm}$. Six lead plates with a total thickness amounting to approximately 120 g/cm^2 were placed in the chambers. The plates were 1, 2, 2.5, 2, 2.5, and 1.5 cm Pb thick respectively. The cloud chamber was placed directly under the master counter groups 5 and 6 (dashed line in Fig. 1). A block diagram of the array is shown in Fig. 2.

For the experimental conditions described above, we calculated the differential spectrum of the showers with respect to the number of particles, the probability of recording the shower cores as a function of the distance from the center of the array, the number of EAS recorded by the given array per unit time, etc. In the calculations it was assumed that:

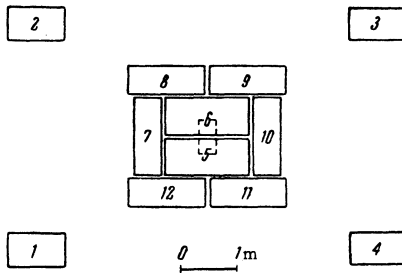


FIG. 1. General diagram of the array.

r(m)	n
0-1	0
1-12	1
12-50	1.5
50-200	2.0
200-500	2.5

(1) EAS possess circular symmetry, and their lateral distribution is independent of the number of particles in the shower and is given by the expression

$$\rho(r) = A_n N / r^n, \quad (1)$$

where N is the number of particles in a shower, the exponent n depends on the distance as in Table I, and $A_n = 1.5 \times 10^{-3}$ for the distance range $1 < r < 12$ m from the axis. The value $n = 0$ for $r < 1$ m, although not corresponding to experimental results,² is caused by the fact that the linear dimensions of each of the master counter groups are larger than 1 m (cf. Fig. 1).

(2) The differential spectrum of showers with respect to the number of particles is of the shape $f(N) dN \sim N^{-(\gamma+1)} dN$, where N is the number of particles in the shower at the observation level, and the dependence of γ on N is that given in reference 3.

(3) The number of axes of EAS with $N > 10^5$ particles, arriving hourly per m^2 at sea level, is $7 \times 10^{-3} m^{-2} \text{ hour}^{-1}$, which corresponds to the data of reference 3.

(4) The distribution of the recording probability of the EAS particles is described by the Poisson law.

The calculated differential size spectra of showers recorded by the given selecting system for $\xi \geq 9$, $\sigma = 330 \text{ cm}^2$ (curves 1 and 2) and $\xi \geq 6$, $\sigma = 100 \text{ cm}^2$ (curves 3 and 4) are shown in Fig. 3. Curves 1 and 3 correspond to showers, the axes of which pass not further than 2 m from the array center, and the curves 2 and 4 correspond to all showers recorded by the array independently of the position of the axes. It can be seen from Fig. 3 that the areas under the curves 1 and 3 are not

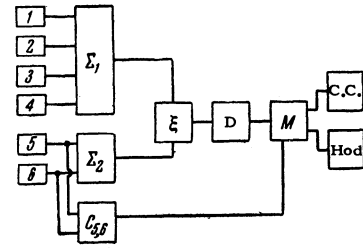


FIG. 2. Block diagram of the array. Σ_1, Σ_2 - circuit producing a pulse proportional to the number of discharged counters in the trays 1 to 4 and 5, 6, respectively; $C_{5,6}$ - double coincidence circuit of the trays 5 and 6; ξ - voltage comparator of circuit for the total pulses from trays 1 to 4 and 5, 6; D - discriminator; M - master pulse shaping; Hod - hodoscope circuit; C.C. - cloud chamber control; 1 to 6 - master counter trays.

much different from the corresponding areas under the curves 2 and 4, indicating a sharp concentration of the cores of recorded showers near the cloud chamber.

A comparison between the experimental and theoretical numbers of recorded EAS and of the mean density of the charged particle flux recorded by the array for $\xi \geq 6$ and $\sigma = 100 \text{ cm}^2$ is given in Table II.

It can be seen from Table II that the results of the calculations are in good agreement with the experiment. This confirms the correctness of the assumptions underlying the calculations.

An advantage of the foregoing triggering system over the often-used triggering by counters connected in coincidence lies in a much greater efficiency of

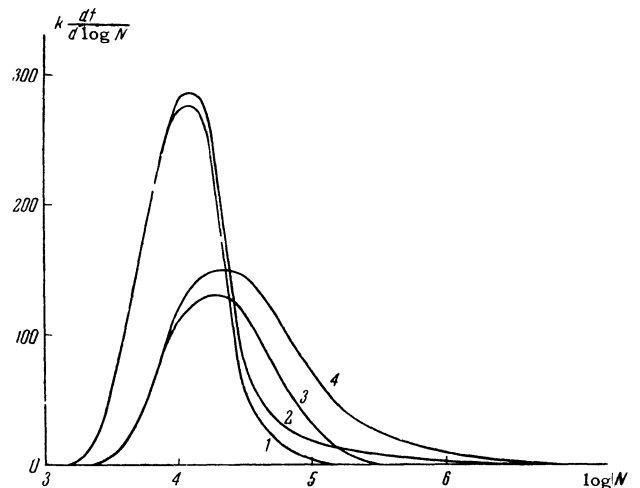


FIG. 3. Calculated differential size spectrum of the showers. The ordinate axis represents $kdf/d \log N$, where k is a proportionality factor. The x axis represents the logarithm of the number of particles in the showers. The normalization is such that the areas under the corresponding curves correspond to the detection efficiency of the cores of the EAS. Curves 1 and 2 - $\xi \geq 9$, $\sigma = 330 \text{ cm}^2$, curves 3, 4 - $\xi \geq 6$, $\sigma = 100 \text{ cm}^2$.

TABLE II

	Experiment	Calculation
Number of particles recorded per hour	2.7 ± 0.2	1-2*
Mean value of the density of particles detected by the array	12 ± 1	10-13

*Best agreement with the experiment is obtained if we assume $A_n \sim 2 \times 10^{-3}$ in Eq. (1).

recording of the axes of EAS. In the given case this is important because of the large dead time of the cloud chamber which sharply diminished the time of measurements and makes it easier to select interesting cases in the reduction of data.

2. EXPERIMENTAL RESULTS

During the operation of the described array we recorded 1800 showers with $\xi \geq 6$, $\sigma = 100 \text{ cm}^2$ and 100 showers with $\xi \geq 9$, $\sigma = 330 \text{ cm}^2$.

A comparison between the experimentally observed and theoretically calculated numbers of the cores of the electron-photon component of EAS passing through the cloud chambers are given in Table III. It can be seen from this table that the experimentally observed and the expected number of cases where the core of the electron-photon component of EAS traversed the cloud chamber are in a good agreement, at least for showers with $N < 3.5 \times 10^4$. If we assume that the energy E_0 of the primary particle initiating the extensive shower

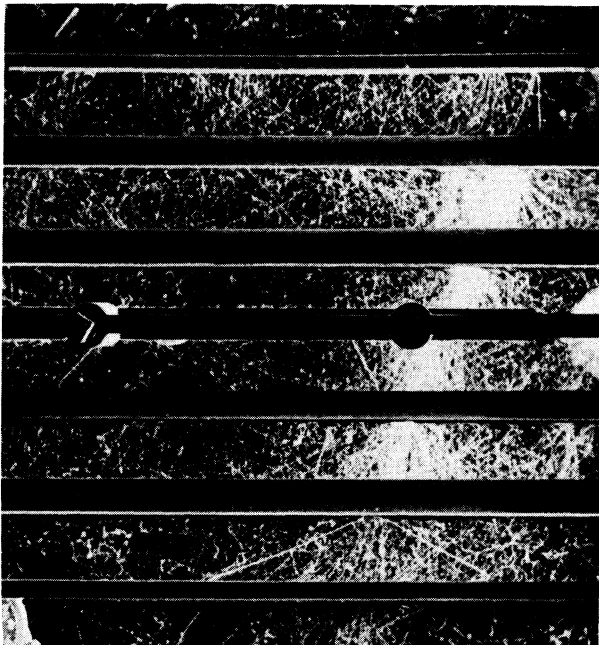


FIG. 5. Nuclear interactions in the lead of the chamber in the 5th and in the 6th plate. The energy of the nuclear-active particle initiating the interaction $\geq 10^{11}$ ev. The number of particles in the EAS is $N = 3.3 \times 10^4$.

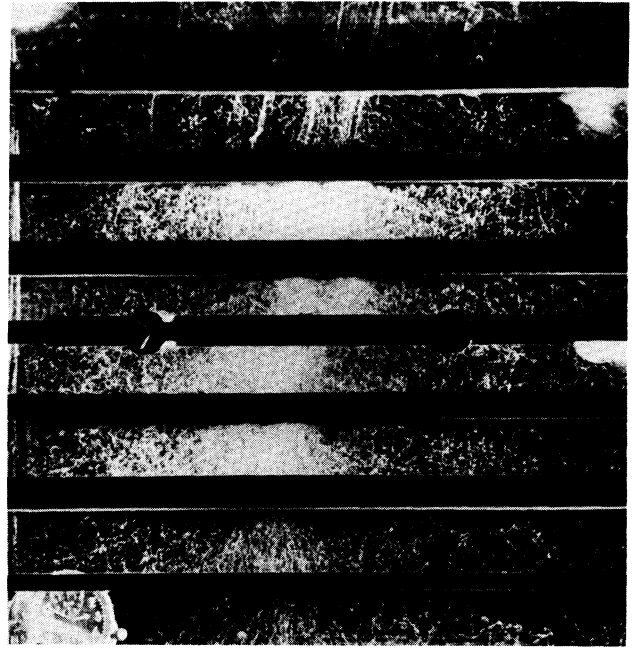


FIG. 4. A photograph of the electron-photon core of an EAS traversing the cloud chamber. The total number of particles in the shower is $N \approx 10^4$ ev.

is proportional to the number of particles in the showers, and that at sea-level $E_0 \approx 1.5 \times 10^{10} N$ ev, then such an energy of the primary particle corresponds to an energy at which, according to the data of reference 5, the structure of the cores of EAS might undergo a change. A photograph of an event in which the electron-photon core of an extensive air shower has traversed the cloud chamber is shown in Fig. 4. This corresponds to a case where a large number of high-energy ($> 10^9$ ev) electrons traverse the chamber simultaneously. It follows from the analysis of the events in which the cores of the electron-photon component traverse the cloud chamber that the high energy electrons are concentrated in a region whose linear dimensions are on the order of 20 or 30 cm, which can be seen in Fig. 4.

If we assume that one nuclear-active particle of $\geq 10^{11}$ ev is present in the core region then, during the time of operation of the array, one should observe in the cloud chamber about five nuclear interactions for showers with a number of particles $N < 3.5 \times 10^4$ and one to two nuclear interactions for showers with $N > 3.5 \times 10^4$. During the total time of operation of the chamber, we observed four nuclear-active particles with energy $\geq 10^{11}$ ev, associated with showers with $N \geq 3.5 \times 10^4$ (cf. Table III).

A characteristic feature of these interactions is the absence of high-energy electrons in their immediate vicinity. This indicates that the nuclear-

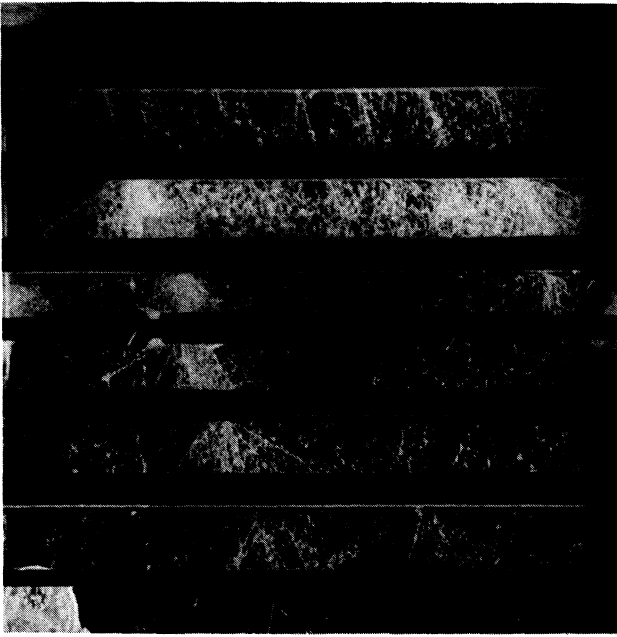


FIG. 6. Nuclear interaction produced by a charged particle in the first plate. The energy of the nuclear particle $\geq 3 \times 10^{11}$ ev. The number of particles in the extensive shower is $N = 2.5 \times 10^4$.

active particle can be present at a certain distance from the core of EAS determined from the electron-photon component.

We shall consider each of these interactions separately.

No. 1 (Fig. 5). Not less than seven particles were produced as a result of a nuclear interaction which took place in the cover of the cloud chamber. Three of these particles underwent nuclear interactions in traversing the lead plates (these interactions could be identified by means of heavy ionizing particles). The energy of the interacting particles can be estimated only for the nuclear-active particles that have undergone nuclear interactions in the top of the chamber and in the sixth plate. If we estimate the energy of nuclear-active particles from the number of secondary penetrating particles and from their angular distribution,⁶ we obtain for the energy of the interaction in the chamber lid a value $E \geq 10^{10}$ ev. Since, however, the energy of the nuclear-active particle initiating a shower in the sixth plate is $E \sim 5 \times 10^{10}$ ev, we must ascribe an energy of $\sim 10^{11}$ ev to the primary particle. The total number of particles in the EAS is $N \sim 3.3 \times 10^4$.

No. 2 (Fig. 6). A nuclear interaction produced by a charged particle occurred in the first plate. As a result, about 15 particles were produced. The majority of these particles lie within a cone with an opening angle not larger than 5° . This corresponds to $\gamma_C \geq 10$, i.e., to an energy of the inci-

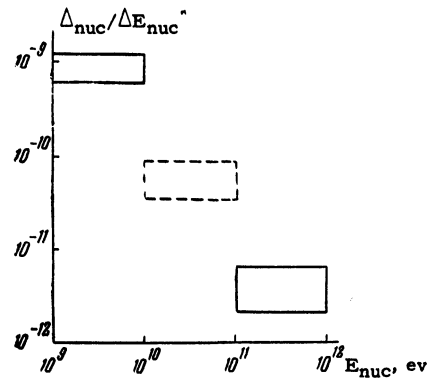


FIG. 7. Differential energy spectrum of the observed nuclear-active particles. The y axis represents the number of nuclear-active particles in the given energy range, and the x axis the energy of nuclear-active particles in electron-volts. The dashed figure indicates the expected number of nuclear-active particles in the energy range 10^{10} to 10^{11} ev.

dent nucleon $E \gtrsim 2 \times 10^{11}$ ev. At least four secondary nuclear-active particles undergo nuclear interactions in traversing the lead plate. It is difficult, however, to estimate their energy because of the large number of secondary electrons.

This interaction is accompanied by a large number of high-energy electrons in spite of a relatively small number of particles in the extensive shower ($N \sim 2.5 \times 10^4$).

No. 3. A nuclear interaction produced by a charged particle in the third plate. The majority of secondary particles are concentrated in a very narrow cone with an opening angle not larger than 5° . The energy of the nuclear-active particle can

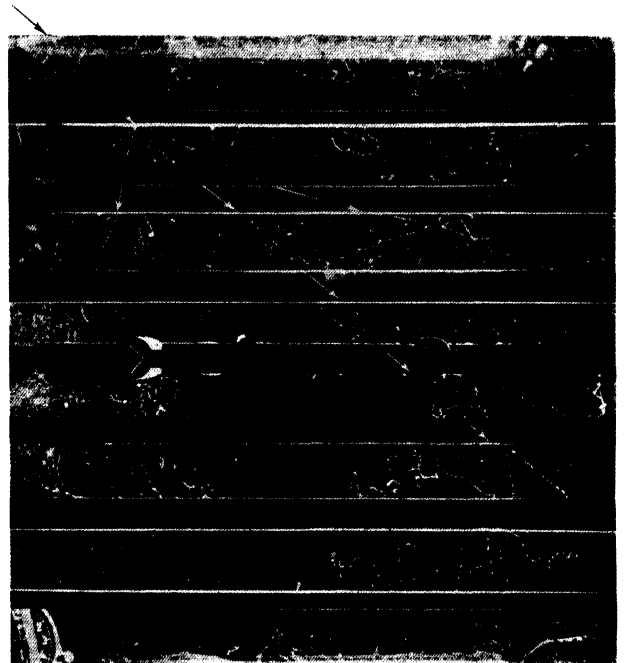


FIG. 8. Nuclear interaction produced by a nuclear-active particle with energy $< 10^{10}$ ev.

be estimated from the maximum of shower development. This occurs at the depth of ~ 10 t-units. If we assume that, in the given interaction, all the energy has been carried away by one π^0 meson, then the energy of the nuclear-active particle is $E \approx 1.5 \times 10^{11}$ ev. This is the lower limit of the energy. If we assume that, in lead, on the average $\sim 20\%$ of the energy of the incident nucleon is carried away by π mesons at interaction energies of 10^{11} to 10^{12} ev, then the energy of the nuclear-active particle initiating the given shower is $\sim (8 \text{ to } 10) \times 10^{11}$ ev.

It should be noted that the total number of particles in this EAS is very small ($N \lesssim 10^4$).

No. 4. An intensive electron-nuclear shower, the energy of which can be estimated only very roughly ($\gtrsim 10^{11}$ ev) because of the large number of high-energy electrons accompanying the nuclear-active particle, can be observed in one of the lower lead plates of the cloud chamber.

3. DISCUSSION OF RESULTS

As has been said above, the theoretically expected number of events in which the cores of EAS with $N < 3.5 \times 10^4$ traversed the cloud chamber, coincides with that observed experimentally. This indicates not only the correctness of the assumption underlying the calculations, but makes it possible to estimate the number of nuclear-active particles of high energy in the core of the shower. The expected and observed numbers of nuclear-interactions produced by these particles in the lead plates of the cloud chamber is given in Table III. These numbers are practically identical for showers with a number of particles $N < 3.5 \times 10^4$. Since it was assumed in the calculation of the expected number of nuclear interactions that only one particle in a given energy range is present in each shower, the agreement between the calculation and the experiment confirms this assumption for showers with $N < 3.5 \times 10^4$. A question arises as to whether the selection of the four cases among the remaining nuclear interaction events was objective. Twelve nuclear interactions were observed during the operation of the cloud chamber.* In eight cases (apart from those described above the energy was estimated by the method given in reference 6. The estimate showed that all the nuclear-active particles have a relatively low energy ($< 10^{10}$ ev).

*One can determine the mean value of the fraction of nuclear-active particles in a shower by using the mean value of the charged particle flux density in the detected showers. This fraction was found to be equal to $(1 \pm 0.3)\%$, which is in agreement with the data of reference 7.

TABLE III

	$N < 3.5 \cdot 10^4$		$N > 3.5 \cdot 10^4$	
	Calculation	Experiment	Calculation	Experiment
Number of cores of the electron-photon component	~ 10	9	~ 3	2
Number of nuclear-active particles with energy 10^{11} ev	~ 5	4	1-2	0

The differential energy spectrum of nuclear-active particles observed in the cloud chamber is given in Fig. 7. It is characteristic that in the energy range of nuclear-active particles, 10^{10} to 10^{11} ev, no nuclear interactions were observed. The probability of such an event is less than 0.05. This feature of the energy spectrum can be explained by errors in the estimate of the energy of nuclear-active particles. A photograph of a nuclear interaction produced by a nuclear-active particle with energy $< 10^{10}$ ev is shown in Fig. 8. A comparison of the particle under consideration and of other nuclear-active particles in the core of EAS. The question arises here as to the role of such a particle in the development of a shower in the depth of the atmosphere. A comparison of the energy of the particles observed by us ($\bar{E} = 2 \times 10^{11}$ ev) with the mean energy carried by the electron-photon component in the same showers ($\sim 2.5 \times 10^{12}$ ev), shows that the energy of one particle is not sufficient in order to change substantially the absorption of the shower and, consequently, a larger part of the secondary electron-photon component is produced in interactions of particles of lower energies. The energy of the particle is, however, fully sufficient for re-initiating the high-energy electron-photon component in the shower core. In fact, it follows from the analysis of the detected cores of EAS that the energy of the nuclear-active particle singled out is of the same order of magnitude as the energy of the electron-photon component in the core of the EAS. It should be noted that the position of the singled-out particle can be somewhat different from the position of the electron-photon component of high-energy and from the axis of the EAS, because of the transverse momenta (μc) gained by secondary particles in the nuclear interactions. Such a core region diffused up to a distance of ~ 1 m, was observed in our experiments, as well as in earlier investigations.²

We shall compare the mean energy of the detected singled-out particles with the energy of the primary particle initiating the EAS. The energy of the primary particle can be found from the total number of shower particles at the observation

level.⁴ For showers with a number of particles 2×10^4 , this amounts to $E_0 = 3 \times 10^{14}$ ev. The mean energy of the four nuclear-active particles detected in the cloud chamber amounts to $\sim 2 \times 10^{11}$ ev. If we assumed that the mean free path for nuclear interactions in air is 70 g/cm^2 , and that we can neglect the fluctuations in the development of EAS, then the energy fraction conserved by these singled-out particles in each nuclear interaction development amounts, on the average, to ~ 0.6 . We have already indicated in the introduction that more accurate quantitative results can be obtained using ionization chambers. It can be concluded from the photographs of cores traversing a cloud chamber that, in the central regions of EAS, high energy nuclear-active particles propagate in close vicinity of each other. In consequence, it is possible and worthwhile to use ionization chambers of sufficiently large dimensions for the study of the energy characteristics of the core of EAS.

In conclusion, the authors consider it their pleasant duty to express their gratitude to Prof. N. A. Dobrotin and G. T. Zatsepin for their interest in the work; to N. G. Birger and D. S. Chernyavskii for the discussion of the results, as well as

to O. A. Kozhevnikov, A. M. Mozhaev, B. V. Subotin, and E. N. Tarasov for their help in carrying out the measurements.

¹E. A. Ivanovskaya and A. G. Novikov, *J. Tech. Phys. (U.S.S.R.)* **26**, 209 (1956), *Soviet Phys. JTP* **1**, 206 (1956).

²O. I. Dovzhenko and S. I. Nikol'skii, *Dokl. Akad. Nauk SSSR* **102**, 241 (1955).

³R. J. Norman, *Proc. Phys. Soc. A* **69**, 443A, 804 (1956).

⁴K. Greisen, *Progress in Cosmic Ray Physics* **III**, Amsterdam (1956).

⁵Nikol'skiĭ, Vavilov, and Batov, *Dokl. Akad. Nauk SSSR* **111**, 71 (1956), *Soviet Phys. "Doklady"* **1**, 625 (1956).

⁶I. A. Ivanovskaya and D. S. Chernavsky, *Nucl. Phys.* **4**, 29 (1956).

⁷Abrosimov, Zatsepin, Solov'eva, Khristiansen, and Chikin, *Izv. Akad. Nauk SSSR, Ser. Fiz.* **19**, 677 (1956) [*Columbia Tech. Transl.* **19**, 616 (1956)].

Translated by H. Kasha